

# Human CtIP promotes DNA end resection

Alessandro A. Sartori<sup>1</sup>, Claudia Lukas<sup>2</sup>, Julia Coates<sup>1</sup>, Martin Mistrik<sup>2</sup>, Shuang Fu<sup>3</sup>, Jiri Bartek<sup>2</sup>, Richard Baer<sup>3</sup>, Jiri Lukas<sup>2</sup> & Stephen P. Jackson<sup>1</sup>

**In the S and G2 phases of the cell cycle, DNA double-strand breaks (DSBs) are processed into single-stranded DNA, triggering ATR-dependent checkpoint signalling and DSB repair by homologous recombination. Previous work has implicated the MRE11 complex in such DSB-processing events. Here, we show that the human CtIP (RBBP8) protein confers resistance to DSB-inducing agents and is recruited to DSBs exclusively in the S and G2 cell-cycle phases. Moreover, we reveal that CtIP is required for DSB resection, and thereby for recruitment of replication protein A (RPA) and the protein kinase ATR to DSBs, and for the ensuing ATR activation. Furthermore, we establish that CtIP physically and functionally interacts with the MRE11 complex, and that both CtIP and MRE11 are required for efficient homologous recombination. Finally, we reveal that CtIP has sequence homology with Sae2, which is involved in MRE11-dependent DSB processing in yeast. These findings establish evolutionarily conserved roles for CtIP-like proteins in controlling DSB resection, checkpoint signalling and homologous recombination.**

DSBs are highly cytotoxic lesions induced by ionizing radiation and certain anti-cancer drugs. They also arise when replication forks encounter other lesions and are generated as intermediates during meiotic recombination<sup>1</sup>. Cells possess two main DSB repair mechanisms: non-homologous end-joining and homologous recombination. Whereas non-homologous end-joining predominates in G0/G1 and is error-prone, homologous recombination is restricted to S and G2, when sister chromatids allow faithful repair<sup>2–4</sup>. Homologous recombination is initiated by resection of DSBs to generate single-stranded DNA (ssDNA) that binds RPA. A ssDNA–RAD51 nucleoprotein filament then forms to initiate strand invasion. ssDNA–RPA also recruits ATR, triggering ATR-dependent checkpoint signalling by the protein kinase CHK1 (also known as CEHK1) (ref. 5). Because DSB resection is largely restricted to S and G2, both homologous recombination and checkpoint signalling by ATR are subject to cell-cycle control<sup>6–8</sup>.

A factor implicated in DSB resection is the MRE11–RAD50–NBS1/NBN (MRN) complex, which binds DNA ends, possesses exo- and endo-nuclease activities and functions in triggering DNA-damage checkpoints<sup>9,10</sup>. Here, we show that human CtIP physically and functionally interacts with MRN. CtIP—initially identified as an interactor for CtBP<sup>11</sup> and the tumour suppressor proteins RB1 (ref. 12) and BRCA1 (refs 13, 14)—is recruited to DNA damage and complexes with BRCA1 to control the G2/M DNA-damage checkpoint<sup>15–17</sup>. We reveal that CtIP also promotes ATR activation and homologous recombination by cooperating with MRN to mediate DSB resection. On the basis of these findings and our identification of sequence homologies between CtIP and Sae2—a protein implicated in mitotic and meiotic DSB processing in *Saccharomyces cerevisiae*<sup>18–22</sup>—we conclude that these proteins are functional homologues.

## CtIP affects cellular responses to DSBs

To investigate CtIP function, we examined how its depletion affected clonogenic survival of human U2OS cells, following their treatment with DNA-damaging agents. To circumvent possible effects arising from CtIP's involvement in controlling cell-cycle progression, we employed acute (1 h) drug treatments rather than continuous drug

exposure. Short interfering (si)RNA-mediated depletion of CtIP caused hypersensitivity towards the topoisomerase I inhibitor camptothecin and the topoisomerase II inhibitor etoposide (Fig. 1a, b) but did not alter cell-cycle distribution profiles and only modestly decreased the proportion of replicating cells (Supplementary Fig. 1a). Furthermore—and consistent with the major cytotoxic lesions caused by camptothecin and etoposide being DSBs arising during S phase<sup>23</sup>—the effects of CtIP depletion were largely abrogated by treating cells with the DNA-replication inhibitor aphidicolin (Fig. 1a, b). These data therefore suggested that CtIP depletion impairs cell survival when DSBs are generated during S phase. Also, because DSBs generated in S phase by camptothecin are repaired by homologous recombination<sup>24</sup>, these results suggested that CtIP promotes homologous recombination. Congruent with CtIP being unnecessary for non-homologous end-joining, its depletion caused only weak hypersensitivity towards bleocin, which generates DSBs at all cell-cycle stages (Fig. 1c, and Supplementary Fig. 1b).

We next assessed the impact of CtIP on phosphorylations mediated by the protein kinases ATM and ATR. In response to DSBs, ATM phosphorylates the checkpoint kinase CHK2 (also known as CHEK2) and histone H2AX (also known as H2AFX; generating a protein species termed  $\gamma$ H2AX)<sup>25,26</sup>. In contrast, ATR activation by ssDNA elicits CHK1 phosphorylation<sup>5</sup>. As shown in Fig. 1d, camptothecin triggered  $\gamma$ H2AX formation and the generation of a slower-migrating, hyper-phosphorylated species of CtIP (CtIP hyper-phosphorylation was demonstrated by phosphatase treatments and a phospho-specific antibody; Supplementary Fig. 1c, d). Furthermore, both CtIP and H2AX phosphorylation were prevented when aphidicolin was co-administered with camptothecin. Etoposide also triggered modification of H2AX and CtIP; however, in this case, CtIP phosphorylation but not H2AX phosphorylation was abrogated by aphidicolin (Fig. 1e). These data are in accord with etoposide being able to generate DSBs throughout the cell cycle, and suggest that CtIP phosphorylation occurs most effectively in S phase.

CtIP depletion did not affect H2AX phosphorylation triggered by either camptothecin or etoposide, revealing that CtIP is not required for DNA-lesion generation by these drugs (Fig. 1d, e). Similarly,

<sup>1</sup>The Wellcome Trust and Cancer Research UK Gurdon Institute, and Department of Zoology, University of Cambridge, Tennis Court Road, Cambridge CB2 1QN, UK. <sup>2</sup>Institute of Cancer Biology and Centre for Genotoxic Stress Research, Danish Cancer Society, Strandboulevarden 49, DK-2100 Copenhagen, Denmark. <sup>3</sup>Institute for Cancer Genetics, Department of Pathology, Columbia University, New York, New York 10032, USA.

camptothecin-induced phosphorylations of CHK2 and SMC1 were unaffected by CtIP depletion, indicating that ATM activation still occurs when CtIP is absent (Fig. 1f, and data not shown). In contrast, CtIP depletion diminished camptothecin-induced CHK1 phosphorylation on Ser 345 and Ser 317 (Fig. 1f, and data not shown). Notably, CtIP depletion markedly impaired CHK1 phosphorylation at late time-points but not at early time-points after continuous camptothecin exposure (Supplementary Fig. 1e). This suggested that CtIP is not required for initial CHK1 phosphorylation triggered by replication stress induced by trapped DNA topoisomerase I molecules, but is needed for signalling of camptothecin-induced replication-dependent DSBs, which, as for ionizing-radiation-induced DSBs<sup>7,27</sup>, might require resection to elicit ATR activation. We reasoned that if this

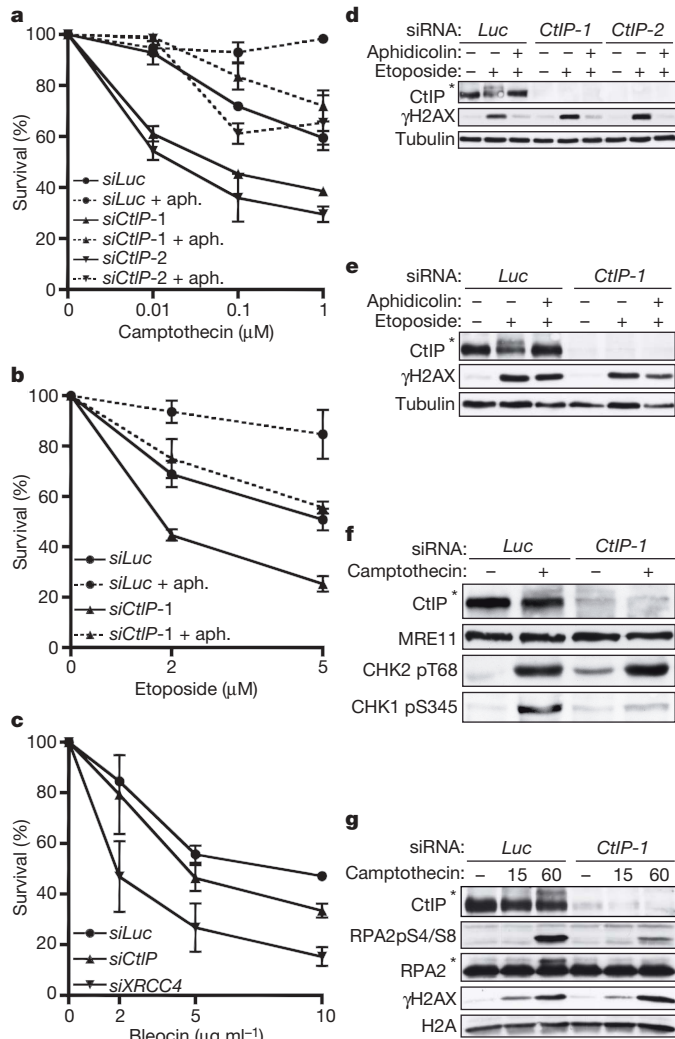


**Figure 1 | CtIP depletion causes hypersensitivity to DSB-inducing agents.** **a–c**, CtIP downregulation causes replication-dependent camptothecin and etoposide hypersensitivity, and weak bleocin hypersensitivity. U2OS cells were pre-incubated with aphidicolin (aph.) where indicated, then treated for 1 h with camptothecin, etoposide or bleocin. *CtIP-1* and *CtIP-2* are two independent siRNAs. siRNAs against Luciferase (siLuc) and XRCC4 (siXRCC4) were used as internal controls and are described in more detail in Supplementary Methods. Survival data represent mean  $\pm$  s.e.m. from  $\geq 3$  independent experiments. **d, e**, Aphidicolin suppresses camptothecin- and etoposide-induced CtIP phosphorylation. Extracts from cells downregulated for luciferase or CtIP and treated with camptothecin or etoposide in the presence or absence of aphidicolin were immunoblotted as indicated. **f, g**, CtIP depletion impairs CHK1 and RPA phosphorylation but not CHK2 phosphorylation after camptothecin treatment. H2A, histone H2A; RPA2pS4/S8 phosphorylation sites are defined in the text. Asterisks in **d–g**: hyper-phosphorylated CtIP and RPA2.

2

was the case, CtIP might influence hyper-phosphorylation of the amino-terminal region of RPA2 by ATM, ATR and DNA-PK (also known as PRKDC) in the context of replication-associated DSBs<sup>28,29</sup>. Indeed, camptothecin-induced RPA2 phosphorylation—as measured by a shift in RPA2 electrophoretic mobility and by phospho-specific antibodies against modified RPA2 serines 4 and 8—was markedly impaired by CtIP depletion, whereas DSB formation, as measured by  $\gamma$ H2AX formation, was unaffected (Fig. 1g). Similarly, CtIP depletion impaired RPA hyper-phosphorylation but not CHK2 or SMC1 phosphorylation in response to etoposide (data not shown). Together, these data indicated that CtIP is required neither for DSB generation by topoisomerase inhibitors nor for DSB detection and signalling by ATM. Instead, CtIP is specifically needed for efficient activation and/or propagation of ATR-mediated signalling.

### CtIP promotes ATR recruitment in S/G2

When we generated DSB-containing tracks in human U2OS cell nuclei by laser micro-irradiation<sup>30</sup>, CtIP was recruited to the damage with kinetics slower than that of  $\gamma$ H2AX formation (Fig. 2a).

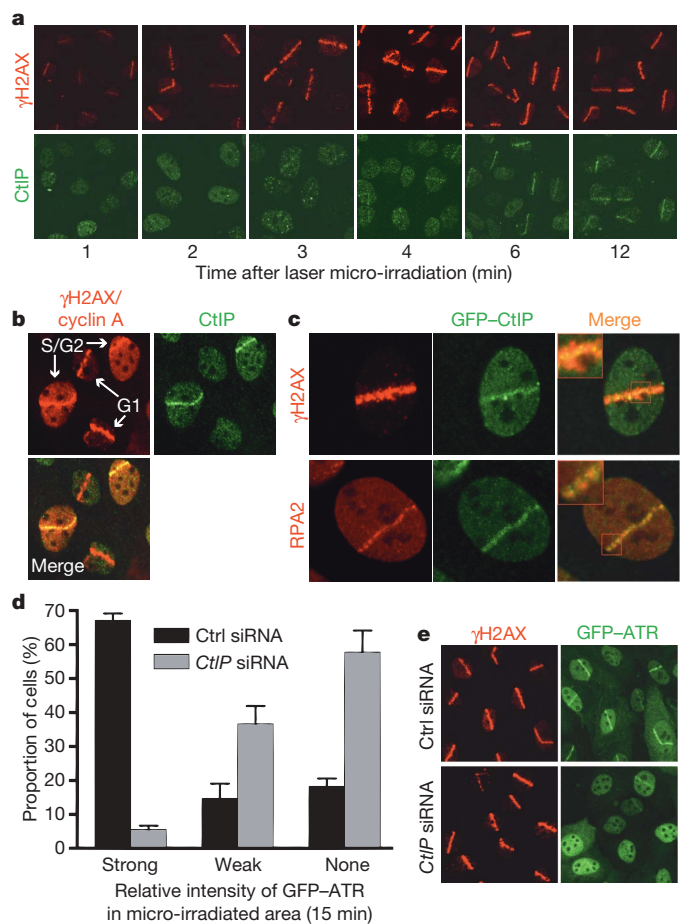


**Figure 2 | CtIP associates with sites of DNA damage in S/G2 phase and promotes ATR recruitment to DSBs.** **a, b**, CtIP recruitment to laser-induced DSBs occurs in S/G2 phase. Cells were stained for endogenous  $\gamma$ H2AX, CtIP or cyclin A. All cells have local  $\gamma$ H2AX signals but only S/G2-phase cells have pan-nuclear cyclin A staining. **c**, GFP-CtIP co-localizes with RPA-ssDNA. Insets: higher magnifications. **d**, CtIP downregulation impairs ATR recruitment to DNA damage. GFP-ATR-expressing cells were treated, micro-irradiated and monitored (Supplementary Fig. 2c). GFP-ATR DSB tracks were manually scored 15 min after micro-irradiation for control (Ctrl) and CtIP-depleted cells (296 and 264 cells, respectively). Data represent mean  $\pm$  s.e.m. from two experiments. **e**, CtIP depletion does not affect  $\gamma$ H2AX formation. Cells from **d** were fixed 15 min after micro-irradiation and immunostained. Wherever used in experiments, images to evaluate cellular responses to laser damage were acquired with a 40 $\times$ /1.2 numerical aperture C-Apochromat objective (Zeiss); the nuclear diameter corresponds to approximately 10  $\mu$ m.

Notably, whereas  $\gamma$ H2AX tracks formed in all irradiated cells, only a subset showed strong CtIP recruitment, indicating that CtIP recruitment might be affected by cell-cycle status. Indeed, significant CtIP redistribution to laser tracks was only observed in cells staining positive for cyclin A, indicating that CtIP responds predominantly to DSBs in S and G2 (Fig. 2b).

In the above studies, we noted that—similar to what has been reported for RPA and ATR<sup>31</sup>—CtIP stripes were narrower than those of  $\gamma$ H2AX. Indeed, when we irradiated a U2OS cell line stably expressing green fluorescent protein (GFP)-tagged CtIP (GFP-CtIP; Supplementary Fig. 2a), GFP-CtIP did not cover the entire  $\gamma$ H2AX-modified chromatin region but localized to smaller compartments that resembled those occupied by RPA (Fig. 2c). Consistent with this, endogenous CtIP co-localized with GFP-ATR (Supplementary Fig. 2b). Because ATR localizes to RPA foci, and because we had found that CtIP promotes ATR activation, we used a cell line expressing functional GFP-ATR<sup>7</sup> to examine whether CtIP is needed for ATR recruitment. Indeed, whereas control cells exhibited strong GFP-ATR recruitment to laser tracks, this response was markedly attenuated in CtIP-depleted cells (Fig. 2d, and Supplementary Fig. 2c; note that the siRNA *CtIP-1* is used here and thereafter). Importantly, parallel immunostaining studies on fixed cells revealed that CtIP depletion impaired ATR recruitment but not  $\gamma$ H2AX formation, implying that CtIP does not affect the extent of laser-induced DNA damage (Fig. 2e). Nevertheless, some residual ATR recruitment was observed in CtIP-depleted cells, indicating either that CtIP stimulates but is not absolutely required for ATR recruitment, or that it is essential for ATR recruitment but that CtIP siRNA-depletion was not complete.

### CtIP facilitates the generation of ssDNA

Recruitment of the ATR-ATRIP complex to DNA damage is mediated by interactions with RPA bound to ssDNA<sup>5,32</sup>. To see whether CtIP might affect ssDNA generation, we analysed DSB-induced RPA focus formation. Strikingly, CtIP depletion dramatically impaired RPA recruitment to laser-induced DNA damage (Fig. 3a; as shown in Supplementary Fig. 2d, this defect was ameliorated when cells stably expressed siRNA-resistant GFP-CtIP, indicating that the GFP-CtIP fusion is functional and that the phenotypes caused by the siRNA are CtIP-dependent). Similarly, camptothecin exposure generated large numbers of RPA foci in control cells (~40% showed this pattern, reflecting the proportion of cells in S phase), whereas CtIP-depleted cells generally lacked detectable RPA foci despite having normal  $\gamma$ H2AX induction (Fig. 3b). Moreover, by using an anti-BrdU antibody staining technique that

only detects DNA in single-stranded form, we found that camptothecin triggered substantial ssDNA formation in control cells but not in CtIP-depleted cells (Fig. 3c, and Supplementary Fig. 3a, b). These data therefore established that CtIP promotes ssDNA formation.

### CtIP interacts with MRN and promotes DNA repair

MRN promotes the processing of DSBs to generate RPA-coated ssDNA, which is needed for ATR recruitment and ensuing CHK1 phosphorylation<sup>7,33,34</sup>. Having found that CtIP was also required for these events, and because BRCA1 and CtIP co-purify with RAD50 in gel-filtration analyses<sup>15</sup>, we examined whether MRN and CtIP interact. Thus, we carried out immunoprecipitations from human HeLa cell nuclear extracts with antisera raised against the C- or N-terminal regions of CtIP. As shown in Fig. 4a, MRN and BRCA1 were detected in CtIP immunoprecipitates. Although most CtIP was recovered by such immunoprecipitations, BRCA1 was only inefficiently retrieved, possibly reflecting the G2-specific nature of the CtIP-BRCA1 interaction<sup>16</sup>. Furthermore, only a proportion of MRN was recovered in CtIP immunoprecipitates, suggesting that there might be different populations of MRN, with only a subset CtIP-associated. The interaction between CtIP and MRN was quite stable, surviving washing in 0.5 M NaCl, and persisted in the presence of ethidium bromide, indicating that it was not DNA-mediated (data not shown). Conversely, CtIP was retrieved in RAD50 and MRE11 immunoprecipitates (Fig. 4b, and data not shown). The CtIP-MRN interaction was unaffected by camptothecin treatment and took place when BRCA1 was depleted (Fig. 4b). Furthermore, when we used extracts from human HCC1937 cells, CtIP was found in RAD50 immunoprecipitates and vice versa (Supplementary Fig. 4a). Because HCC1937 cells express low levels of functionally impaired BRCA1 bearing a mutation in its C-terminal tandem BRCT domain that precludes its interaction with CtIP<sup>16</sup>, these data implied that BRCA1 does not bridge the CtIP-MRN interaction. Indeed, CtIP co-immunoprecipitated with RAD50 from mixtures containing only purified, recombinant CtIP and MRN, demonstrating a direct interaction between the two factors (Supplementary Fig. 4b).

To characterize the CtIP-MRN interaction further, we expressed in bacteria various regions of CtIP fused to glutathione S-transferase (GST) and assessed their ability to retrieve MRN complexes from HeLa nuclear extracts (Fig. 4c). Whereas MRN did not bind to N-terminal regions of CtIP containing a putative coiled-coil or the BRCA1 interaction motif<sup>16</sup> (lanes 4 and 5), it bound efficiently when GST was fused to full-length CtIP or to a region comprising the C-terminal 108 residues of CtIP (lanes 3 and 7; see Supplementary Fig. 6a for a schematic view of the CtIP fragments). Furthermore,

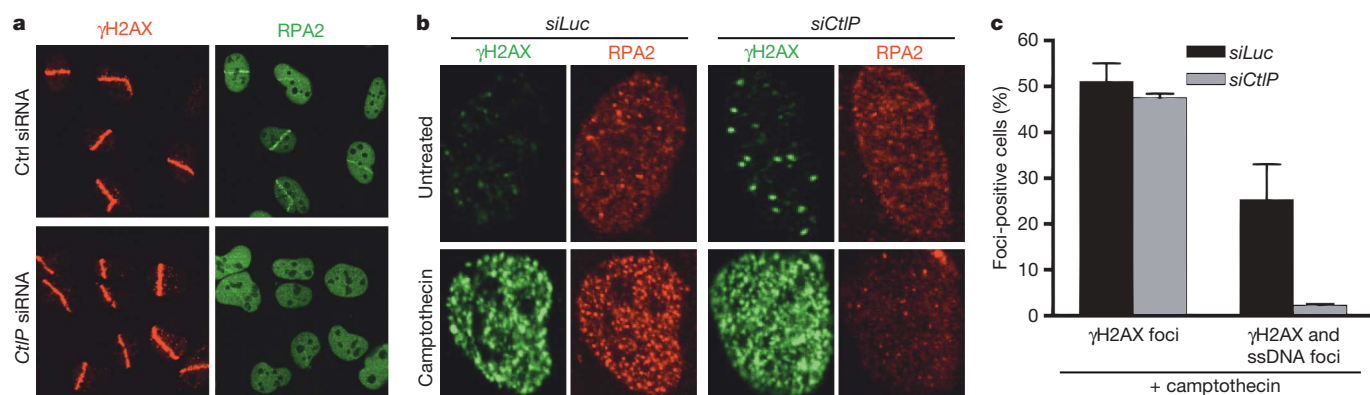


**Figure 3 | CtIP depletion impairs DSB resection.** **a, b**, CtIP is required for RPA recruitment to laser- and CPT-induced DSBs. Cells treated with control or CtIP siRNA were either micro-irradiated and 30 min later co-immunostained for  $\gamma$ H2AX and RPA2, or were treated with camptothecin for 1 h and immunostained. **c**, CtIP depletion impairs ssDNA formation. After siRNA treatment, cells were tested for camptothecin-induced ssDNA

formation by a non-denaturing BrdU staining procedure (see Methods and text for details). For each camptothecin-treated sample, >100 cells were counted and the percentage exhibiting  $\gamma$ H2AX foci, or both  $\gamma$ H2AX and ssDNA foci, was determined (Supplementary Fig. 3a, b). Data represent the mean  $\pm$  s.e.m. from two independent experiments.

when we used purified GST-fusions of CtIP (expressed in bacteria or insect cells), they bound directly to purified, baculovirus-expressed human MRE11–RAD50 (Supplementary Fig. 4c,d). However, whereas GST-fusions containing the CtIP C-terminal region interacted with MRE11–RAD50 (Supplementary Fig. 4c), a GST–CtIP fusion lacking the CtIP C-terminal region still interacted with MRE11–RAD50 (Supplementary Fig. 4d). These data therefore indicated that CtIP and MRN interact directly and that there is more than one point-of-contact between the two factors.

Because both CtIP and MRE11 are needed for effective DSB resection, we speculated that CtIP might affect nuclease activities associated with the MRE11 complex<sup>10,35–37</sup>. Thus, we expressed CtIP in insect cells, purified it to homogeneity (Supplementary Fig. 4b) and used it together with purified MRE11–RAD50 in an endonuclease assay with closed-circular single-stranded PhiX174 DNA (Fig. 4d). As shown previously<sup>38</sup>, MRE11–RAD50 exhibited nuclease activity in the presence of manganese (lane 12) but not in the presence of magnesium (lane 5). In contrast, CtIP did not show detectable nuclease activity with either metal cofactor (lanes 3 and 10). Strikingly, when CtIP was combined with MRE11–RAD50, this produced endonuclease activity in the presence of magnesium (lane 6) and produced more endonuclease activity in the presence of manganese than was exhibited by MRE11–RAD50 alone (compare lanes 12 and 13). Heat denaturation of CtIP abolished its stimulatory effects and ATP was required neither for MRE11–RAD50 activity nor for the stimulatory effect of CtIP (data not shown). Notably, when we carried out MRE11–RAD50-dependent exonuclease assays with short (50 bp) radiolabelled oligonucleotide substrates, however, we did not detect CtIP-dependent effects (data not shown). We therefore speculate that CtIP mainly promotes endo- but not exonucleolytic activities in conjunction with the MRE11 complex.

Given that both CtIP and MRN regulate DSB resection, we speculated that they might facilitate homologous recombination. To address this, we used a U2OS cell line bearing one or two copies of an integrated homologous recombination reporter composed of two differentially mutated GFP genes oriented as direct repeats. Transient expression of I-SceI endonuclease in such cells generates a DSB that, when repaired by gene conversion, results in a functional GFP gene, the expression of which can be assessed by flow cytometry (Supplementary Fig. 5a)<sup>39</sup>. Significantly, depletion of CtIP or MRE11 decreased homologous recombination frequencies to levels similar to those achieved by depleting the key homologous recombination protein RAD51 (Fig. 4e, and Supplementary Fig. 5b). Furthermore, depleting CtIP and MRE11 together did not decrease homologous recombination efficiency further than was achieved by CtIP or MRE11 depletion alone. These findings therefore revealed that both CtIP and MRE11 promote homologous recombination, and furthermore suggested that they do so through a common mechanism.

### CtIP has homology to *Saccharomyces cerevisiae* Sae2

Prompted by the above findings, we used regions of CtIP in PSI-BLAST-based database searches<sup>40</sup>. Although most regions of CtIP identified related proteins only in higher eukaryotes, we identified proteins in a diverse range of eukaryotes that show homology with the C-terminal 108 amino acid region of CtIP (Supplementary Fig. 6a). Most strikingly, the only *S. cerevisiae* protein identified in this search was Sae2, a protein that genetically interacts with yeast Mre11 to govern camptothecin sensitivity and DSB processing (Fig. 5a, and Supplementary Fig. 6a)<sup>18–22,41,42</sup>. To address the potential functional importance of the CtIP/Sae2 homology region, we generated a U2OS cell line stably expressing an siRNA-resistant GFP-tagged CtIP derivative (residues 1–789) lacking the C-terminal region. Analysis of

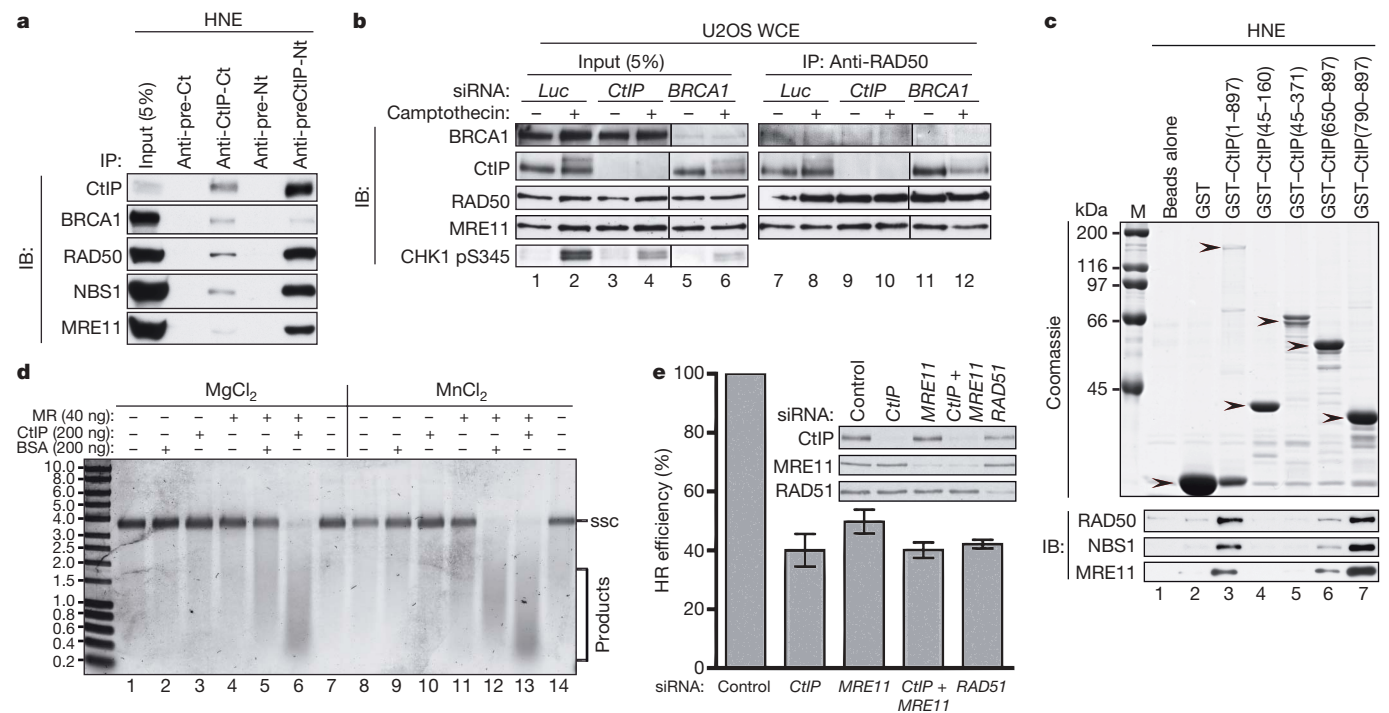


**Figure 4 | CtIP interacts with MRN and promotes homologous recombination.** **a**, MRN co-immunoprecipitates with CtIP. HeLa nuclear extract (HNE) was immunoprecipitated (IP) with pre-immune (pre) or anti-CtIP antibodies (see Supplementary Methods and text for details) and analysed by immunoblotting (IB). **b**, CtIP–MRN interaction after DNA damage and after BRCA1-depletion. Where indicated, cells were treated with 1  $\mu$ M CPT for 1 h. Whole-cell extracts (WCE) were immunoblotted directly or after immunoprecipitation. **c**, The CtIP C terminus binds MRN. Bacterially expressed fusions (arrowheads) were tested for binding MRN in

HNE by immunoblotting. **d**, CtIP stimulates MRE11–RAD50-dependent nuclease activity. PhiX174 substrate was incubated with MRE11–RAD50 (MR; 40 ng), BSA (200 ng) or CtIP (200 ng) in 5 mM MgCl<sub>2</sub> or MnCl<sub>2</sub>, run on an agarose gel and stained with SYBR Gold. A series of size markers (in kb) is indicated on the left. ssc, circular ssDNA. **e**, CtIP or MRE11 downregulation impairs homologous recombination (see Methods and text for details). Data represent the mean  $\pm$  s.e.m. from four independent experiments. HR, homologous recombination.

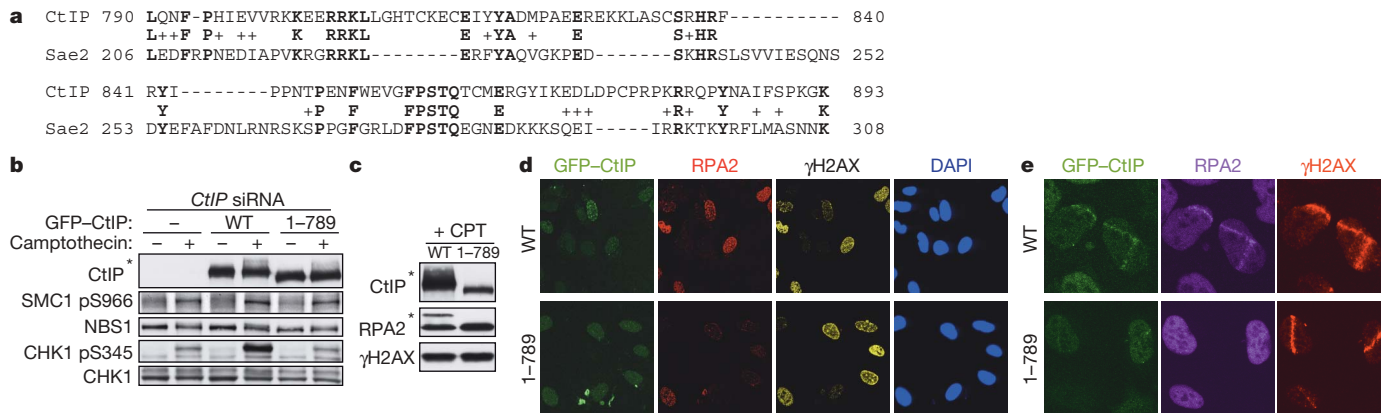


**Figure 5 | Function and evolutionary conservation of the CtIP C terminus.** **a**, Alignment of CtIP and Sae2 arising from BLAST-searches with the CtIP C terminus (790–897). **b–e**, Deletion of the CtIP C terminus impairs CtIP function. Three days after siRNA transfection, U2OS cells stably expressing GFP-tagged siRNA-resistant wild-type CtIP (WT) or a deletion mutant

(1–789) were either treated with 1  $\mu$ M CPT for 1 h and analysed by immunoblotting or co-immunostaining, or were micro-irradiated and 30 min later co-immunostained as indicated. Asterisks in **b** and **c**: hyperphosphorylated CtIP and RPA2.

these cells under conditions where the endogenous CtIP protein was downregulated established that, unlike the wild-type protein, the CtIP truncation mutant did not promote efficient CHK1 phosphorylation, RPA2 hyper-phosphorylation or RPA focus formation on camptothecin treatment (Fig. 5b–d). Similarly, wild-type CtIP promoted the formation of RPA-coated ssDNA in laser micro-irradiation studies, whereas the CtIP C-terminal truncation mutant did not (Fig. 5e; a similar proportion of wild-type and mutant cells stained positive for cyclin A, ruling out cell-cycle effects—data not shown). As anticipated from previous experiments (Supplementary Fig. 4d), both wild-type CtIP and the truncation mutant could be co-immunoprecipitated with RAD50 (Supplementary Fig. 6b). Taken together, these data therefore indicated that the conserved C-terminal region of CtIP is functionally important.

## Discussion

We have shown that CtIP facilitates DSB resection and ssDNA formation, thus activating the ATR/CHK1 axis of the DNA-damage response and DNA repair by homologous recombination. Consequently, cells depleted of CtIP show hypersensitivity towards DSB-inducing agents, particularly those that generate DSBs specifically in S phase. Furthermore, we have established that CtIP functionally interacts with the MRN complex. Taken together with the fact that MRN also promotes DSB resection, ATR signalling and homologous recombination, these findings identify CtIP as a critical regulator of the checkpoint signalling and DNA repair functions of the MRN complex.

We have also found that the CtIP C terminus is highly conserved in CtIP orthologues in other organisms and is required for CtIP function in human cells. Strikingly, this domain shows homology with the C terminus of *S. cerevisiae* Sae2, which genetically cooperates with the yeast Mre11 complex to promote DSB resection. We therefore conclude that CtIP and Sae2 are probably functional counterparts and that proteins related to these factors will turn out to control DSB resection, ssDNA-mediated checkpoint signalling and homologous recombination in diverse eukaryotes. Efficient DSB processing is restricted to S and G2 phases, and requires CDK and ATM kinase activity<sup>7</sup>. It is therefore noteworthy that CtIP and Sae2 are phosphorylated by ATM and the yeast counterpart of ATR<sup>43–45</sup>, respectively, and that the CtIP/Sae2 homology region contains conserved potential CDK and ATM/ATR target sites. This raises the exciting possibility that phosphorylation of these sites regulates DSB resection. In addition, CtIP interacts with and is ubiquitinated by BRCA1 (refs 13, 14, 16, 17), and has been identified as an RB1 interaction-partner<sup>12</sup>, suggesting that these interactions might control the fate of DSBs during the cell cycle. Finally, it is significant that CtIP governs

responses to commonly used anti-cancer agents and that CtIP alterations have been reported in some cancer cells, thus highlighting CtIP and its interaction with MRN as potential targets for drug discovery<sup>13,46,47</sup>.

## METHODS SUMMARY

HeLa, HCC1937, U2OS and U2OS-derived cells were cultured in Dulbecco's modified Eagle's medium (DMEM) supplemented with 10% fetal bovine serum (FBS) and standard antibiotics. Data for survival curves were generated by colony formation assays. In brief, U2OS cells were transfected with siRNA (see Supplementary Methods) and treated with DNA-damage-inducing drugs. After 1 h, the drug was removed and cells were left for 10–14 days at 37 °C to allow colonies to form. Colonies were stained with 0.5% crystal violet/20% ethanol and counted. Where indicated, cells were pre-incubated with aphidicolin (10  $\mu$ M) for 90 min, then treated with the specified drug and aphidicolin for 1 h. A U2OS-derived cell line stably expressing GFP-ATR was described previously<sup>7</sup>. The siRNA-resistant silent wild-type GFP-CtIP construct was generated by sub-cloning the CtIP complementary DNA into the pEGFP-C1 expression plasmid (BD Biosciences Clontech) and changing three nucleotides in the CtIP-1 siRNA targeting region by using a QuikChange site-directed mutagenesis kit (Stratagene), as previously described<sup>16</sup>. The plasmid expressing the CtIP mutant lacking the C terminus (1–789) was generated by changing residues 790 and 791 in the wild-type GFP-CtIP construct to two stop-codons. For generation of cell lines stably expressing siRNA-resistant GFP-tagged wild-type and mutant CtIP, U2OS cells were transfected with the appropriate constructs and, following antibiotic selection, resistant clones were tested for expression and nuclear localization of the transgene-product by immunofluorescence microscopy. To detect ssDNA by microscopy, cells were cultivated for 24 h in medium supplemented with 10  $\mu$ M BrdU before camptothecin treatment and, after fixation, immunostained with an anti-BrdU antibody (see Methods) without any preceding DNA denaturation or nuclease treatment<sup>48</sup>. Laser micro-irradiation was performed as described previously<sup>30,31</sup>. Recombinant Flag-GST-CtIP-6H was isolated from baculovirus-infected Sf9 cells as described previously<sup>49</sup>. Recombinant MRE11-RAD50 and MRE11-RAD50-NBS1 (MRN) complex were gifts from T. Paull.

**Full Methods** and any associated references are available in the online version of the paper at [www.nature.com/nature](http://www.nature.com/nature).

Received 24 April; accepted 5 October 2007.

Published online 28 October 2007.

- Wyman, C. & Kanaar, R. DNA double-strand break repair: all's well that ends well. *Annu. Rev. Genet.* **40**, 363–383 (2006).
- Lieber, M. R., Ma, Y., Pannicke, U. & Schwarz, K. Mechanism and regulation of human non-homologous DNA end-joining. *Nature Rev. Mol. Cell Biol.* **4**, 712–720 (2003).
- West, S. C. Molecular views of recombination proteins and their control. *Nature Rev. Mol. Cell Biol.* **4**, 435–445 (2003).
- Sung, P. & Klein, H. Mechanism of homologous recombination: mediators and helicases take on regulatory functions. *Nature Rev. Mol. Cell Biol.* **7**, 739–750 (2006).

5. Zou, L. & Elledge, S. J. Sensing DNA damage through ATRIP recognition of RPA-ssDNA complexes. *Science* **300**, 1542–1548 (2003).
6. Ira, G. *et al.* DNA end resection, homologous recombination and DNA damage checkpoint activation require CDK1. *Nature* **431**, 1011–1017 (2004).
7. Jazayeri, A. *et al.* ATM- and cell cycle-dependent regulation of ATR in response to DNA double-strand breaks. *Nature Cell Biol.* **8**, 37–45 (2006).
8. Aylon, Y., Liefshitz, B. & Kupiec, M. The CDK regulates repair of double-strand breaks by homologous recombination during the cell cycle. *EMBO J.* **23**, 4868–4875 (2004).
9. Lavin, M. F. The Mre11 complex and ATM: a two-way functional interaction in recognising and signaling DNA double strand breaks. *DNA Repair (Amst.)* **3**, 1515–1520 (2004).
10. D'Amours, D. & Jackson, S. P. The Mre11 complex: at the crossroads of DNA repair and checkpoint signalling. *Nature Rev. Mol. Cell Biol.* **3**, 317–327 (2002).
11. Schaeper, U., Subramanian, T., Lim, L., Boyd, J. M. & Chinnadurai, G. Interaction between a cellular protein that binds to the C-terminal region of adenovirus E1A (CtBP) and a novel cellular protein is disrupted by E1A through a conserved PLDL motif. *J. Biol. Chem.* **273**, 8549–8552 (1998).
12. Fusco, C., Reymond, A. & Zervos, A. S. Molecular cloning and characterization of a novel retinoblastoma-binding protein. *Genomics* **51**, 351–358 (1998).
13. Wong, A. K. C. *et al.* Characterization of a carboxy-terminal BRCA1 interacting protein. *Oncogene* **17**, 2279–2285 (1998).
14. Yu, X., Wu, L. C., Bowcock, A. M., Aronheim, A. & Baer, R. The C-terminal (BRCT) domains of BRCA1 interact *in vivo* with CtIP, a protein implicated in the CtBP pathway of transcriptional repression. *J. Biol. Chem.* **273**, 25388–25392 (1998).
15. Greenberg, R. A. *et al.* Multifactorial contributions to an acute DNA damage response by BRCA1/BARD1-containing complexes. *Genes Dev.* **20**, 34–46 (2006).
16. Yu, X. & Chen, J. DNA damage-induced cell cycle checkpoint control requires CtIP, a phosphorylation-dependent binding partner of BRCA1 C-terminal domains. *Mol. Cell Biol.* **24**, 9478–9486 (2004).
17. Yu, X., Fu, S., Lai, M., Baer, R. & Chen, J. BRCA1 ubiquitinates its phosphorylation-dependent binding partner CtIP. *Genes Dev.* **20**, 1721–1726 (2006).
18. McKee, A. H. & Kleckner, N. A general method for identifying recessive diploid-specific mutations in *Saccharomyces cerevisiae*, its application to the isolation of mutants blocked at intermediate stages of meiotic prophase and characterization of a new gene *SAE2*. *Genetics* **146**, 797–816 (1997).
19. Prinz, S., Amon, A. & Klein, F. Isolation of *COM1*, a new gene required to complete meiotic double-strand break-induced recombination in *Saccharomyces cerevisiae*. *Genetics* **146**, 781–795 (1997).
20. Rattray, A. J., McGill, C. B., Shafer, B. K. & Strathern, J. N. Fidelity of mitotic double-strand-break repair in *Saccharomyces cerevisiae*: a role for *SAE2/COM1*. *Genetics* **158**, 109–122 (2001).
21. Lobachev, K. S., Gordenin, D. A. & Resnick, M. A. The Mre11 complex is required for repair of hairpin-capped double-strand breaks and prevention of chromosome rearrangements. *Cell* **108**, 183–193 (2002).
22. Clerici, M., Mantiero, D., Lucchini, G. & Longhese, M. P. The *S. cerevisiae* Sae2 protein promotes resection and bridging of double-strand break ends. *J. Biol. Chem.* **280**, 38631–38638 (2005).
23. D'Arpa, P., Beardmore, C. & Liu, L. F. Involvement of nucleic acid synthesis in cell killing mechanisms of topoisomerase poisons. *Cancer Res.* **50**, 6919–6924 (1990).
24. Saleh-Gohari, N. *et al.* Spontaneous homologous recombination is induced by collapsed replication forks that are caused by endogenous DNA single-strand breaks. *Mol. Cell Biol.* **25**, 7158–7169 (2005).
25. Shiloh, Y. ATM and related protein kinases: safeguarding genome integrity. *Nature Rev. Cancer* **3**, 155–168 (2003).
26. Bakkenist, C. J. & Kastan, M. B. Initiating cellular stress responses. *Cell* **118**, 9–17 (2004).
27. Cuadrado, M. *et al.* ATM regulates ATR chromatin loading in response to DNA double-strand breaks. *J. Exp. Med.* **203**, 297–303 (2006).
28. Shao, R.-G. *et al.* Replication-mediated DNA damage by camptothecin induces phosphorylation of RPA by DNA-dependent protein kinase and dissociates RPA:DNA-PK complexes. *EMBO J.* **18**, 1397–1406 (1999).
29. Sakasai, R. *et al.* Differential involvement of phosphatidylinositol 3-kinase-related protein kinases in hyperphosphorylation of replication protein A2 in response to replication-mediated DNA double-strand breaks. *Genes Cells* **11**, 237–246 (2006).
30. Lukas, C., Falck, J., Bartkova, J., Bartek, J. & Lukas, J. Distinct spatiotemporal dynamics of mammalian checkpoint regulators induced by DNA damage. *Nature Cell Biol.* **5**, 255–260 (2003).
31. Bekker-Jensen, S. *et al.* Spatial organization of the mammalian genome surveillance machinery in response to DNA strand breaks. *J. Cell Biol.* **173**, 195–206 (2006).
32. Ball, H. L., Myers, J. S. & Cortez, D. ATRIP binding to RPA-ssDNA promotes ATR-ATRIP localization but is dispensable for Chk1 phosphorylation. *Mol. Biol. Cell* **16**, 2372–2381 (2005).
33. Adams, K. E., Medhurst, A. L., Dart, D. A. & Lakin, N. D. Recruitment of ATR to sites of ionising radiation-induced DNA damage requires ATM and components of the MRN protein complex. *Oncogene* **25**, 3894–3904 (2006).
34. Myers, J. S. & Cortez, D. Rapid activation of ATR by ionizing radiation requires ATM and Mre11. *J. Biol. Chem.* **281**, 9346–9350 (2006).
35. Paull, T. T. & Gellert, M. The 3' to 5' exonuclease activity of Mre11 facilitates repair of DNA double-strand breaks. *Mol. Cell* **1**, 969–979 (1998).
36. Assenmacher, N. & Hopfner, K. P. MRE11/RAD50/NBS1: complex activities. *Chromosoma* **113**, 157–166 (2004).
37. Larson, E. D., Cummings, W. J., Bednarski, D. W. & Maizels, N. MRE11/RAD50 cleaves DNA in the AID/UNG-Dependent Pathway of immunoglobulin gene diversification. *Mol. Cell* **20**, 367–375 (2005).
38. Trujillo, K. M., Yuan, S.-S. F., Lee, E.-Y. P. & Sung, P. Nuclease activities in a complex of human recombination and DNA repair factors Rad50, Mre11, and p95. *J. Biol. Chem.* **273**, 21447–21450 (1998).
39. Pierce, A. J., Hu, P., Han, M., Ellis, N. & Jasin, M. Ku DNA end-binding protein modulates homologous repair of double-strand breaks in mammalian cells. *Genes Dev.* **15**, 3237–3242 (2001).
40. Schaffer, A. A. *et al.* Improving the accuracy of PSI-BLAST protein database searches with composition-based statistics and other refinements. *Nucleic Acids Res.* **29**, 2994–3005 (2001).
41. Deng, C., Brown, J. A., You, D. & Brown, J. M. Multiple endonucleases function to repair covalent topoisomerase I complexes in *Saccharomyces cerevisiae*. *Genetics* **170**, 591–600 (2005).
42. Lisby, M., Barlow, J. H., Burgess, R. C. & Rothstein, R. Choreography of the DNA damage response: spatiotemporal relationships among checkpoint and repair proteins. *Cell* **118**, 699–713 (2004).
43. Li, S. *et al.* Functional link of BRCA1 and ataxia telangiectasia gene product in DNA damage response. *Nature* **13**, 210–215 (2000).
44. Baroni, E., Viscardi, V., Cartagena-Lirola, H., Lucchini, G. & Longhese, M. P. The functions of budding yeast Sae2 in the DNA damage response require Mec1- and Tel1-dependent phosphorylation. *Mol. Cell Biol.* **24**, 4151–4165 (2004).
45. Cartagena-Lirola, H., Guerini, I., Viscardi, V., Lucchini, G. & Longhese, M. P. Budding yeast Sae2 is an *in vivo* target of the Mec1 and Tel1 checkpoint kinases during meiosis. *Cell Cycle* **5**, 1549–1559 (2006).
46. Vilkki, S. *et al.* Screening for microsatellite instability target genes in colorectal cancers. *J. Med. Genet.* **39**, 785–789 (2002).
47. Wu, G. & Lee, W. H. CtIP, a multivalent adaptor connecting transcriptional regulation, checkpoint control and tumor suppression. *Cell Cycle* **5**, 1592–1596 (2006).
48. Raderschall, E., Golub, E. I. & Haaf, T. Nuclear foci of mammalian recombination proteins are located at single-stranded DNA regions formed after DNA damage. *Proc. Natl Acad. Sci. USA* **96**, 1921–1926 (1999).
49. Wu-Baer, F., Lagrazon, K., Yuan, W. & Baer, R. The BRCA1/BARD1 heterodimer assembles polyubiquitin chains through an unconventional linkage involving lysine residue K6 of ubiquitin. *J. Biol. Chem.* **278**, 34743–34746 (2003).

**Supplementary Information** is linked to the online version of the paper at [www.nature.com/nature](http://www.nature.com/nature).

**Acknowledgements** We thank T. Paull and J. Falck for providing reagents, and P. Huertas, A. Meier, K. Dry, K. Miller and Y. Pommier for advice and critical reading of the manuscript. This study was supported by Cancer Research UK, the EU and a Swiss National Science Foundation fellowship for advanced researcher (A.A.S.). Research in the S.P.J. laboratory is made possible by core infrastructure funding from Cancer Research UK and the Wellcome Trust. C.L., J.L., M.M. and J.B. were supported by grants from the Danish Cancer Society, Danish National Research Foundation, EU (DNA Repair), and the John and Birthe Meyer Foundation and the Czech Ministry of Education. Research in the laboratory of R.B. is supported by the National Institute of Health and S.F. is supported by a fellowship from the New York State Breast Cancer Research Fund.

**Author Contributions** S.F. and R.B. generated CtIP cDNA, CtIP antibodies and recombinant CtIP protein. C.L., J.L., M.M. and J.B. generated the cell lines with GFP-tagged proteins, conceived, performed and evaluated the real-time imaging experiments, and performed the homologous recombination measurements. All other experiments were conceived by A.A.S. and S.P.J., and were performed by A.A.S. with the help of J.C. A.A.S. and S.P.J. wrote the paper. All authors discussed the results and commented on the manuscript.

**Author Information** Reprints and permissions information is available at [www.nature.com/reprints](http://www.nature.com/reprints). Correspondence and requests for materials should be addressed to S.P.J. ([s.jackson@gurdon.cam.ac.uk](mailto:s.jackson@gurdon.cam.ac.uk)).

## METHODS

**Immunofluorescence microscopy.** U2OS cells were transfected with siRNA and after 3 days were treated with 1  $\mu$ M camptothecin (CPT) for 1 h. After pre-extraction for 5 min on ice (25 mM Hepes 7.4, 50 mM NaCl, 1 mM EDTA, 3 mM MgCl<sub>2</sub>, 300 mM sucrose and 0.5% TritonX-100), cells were fixed with 4% formaldehyde (w/v) in PBS for 12 min. Coverslips were washed with PBS and then co-immunostained with primary antibodies against  $\gamma$ H2AX (rabbit polyclonal, Cell Signalling Technology) either in combination with an antibody against RPA2 (mouse monoclonal, Lab Vision) or BrdU (mouse monoclonal, GE Healthcare). Appropriate Alexa Fluor-488 (green) and -594 (red) conjugated secondary antibodies (1:1,000) were purchased from Molecular Probes. Slides were viewed with a Bio-Rad confocal laser microscope by sequential scanning of the two emission channels used.

**Immunoblotting.** Cell extracts were prepared in Laemmli buffer (4% SDS, 20% glycerol, 120 mM Tris-HCl pH 6.8), proteins were resolved by SDS-PAGE and transferred to nitrocellulose. Immunoblots were performed by using the appropriate antibodies (see Supplementary Methods).

**Immunoprecipitation.** If not specified otherwise, cells were lysed in RIPA buffer (50 mM Tris-HCl, pH 7.4, 1% NP-40, 0.25% Na-deoxycholate, 150 mM NaCl, 1 mM EDTA and 0.1% SDS), supplemented with phosphatase inhibitor cocktails 1 and 2 (Sigma) and with complete protease inhibitor cocktail (Roche). Clarified extracts were pre-cleared with protein A or protein G beads (Sigma) for 1 h at 4 °C. Immunoprecipitating antibodies were added to the pre-cleared supernatant and incubated for 2 h at 4 °C. After a 1 h incubation with protein A or protein G beads, precipitated immunocomplexes were washed four times in lysis buffer (containing 0.5% NP-40, without SDS), boiled in SDS sample buffer and loaded on an SDS-polyacrylamide gel. Proteins were analysed by immunoblotting, as described above.

**GST pull-downs.** GST-CtIP fragments were constructed by cloning polymerase chain reaction products into pGEX-4T1 (Amersham). GST fusion plasmids were grown in BL21 RIL (Codon+) *Escherichia coli* (Stratagene) and protein was expressed by incubation for 4 h at 30 °C after the addition of 100  $\mu$ M IPTG. Proteins were purified from soluble extracts with glutathione Sepharose 4 fast flow beads (Amersham). GST fusion proteins bound to glutathione beads were mixed with 1 mg of HeLa nuclear extract and incubated for 1 h at 4 °C in 1 ml of TEN100 buffer (20 mM Tris-HCl, pH 7.4, 0.1 mM EDTA and 100 mM NaCl). Beads were then washed four times with NTEN300 buffer (0.5% NP-40, 0.1 mM EDTA, 20 mM Tris-HCl, pH 7.4, 300 mM NaCl), complexes were boiled in SDS sample buffer and analysed by SDS-PAGE followed by either Coomassie staining or immunoblotting.

**In vitro nuclease assay.** The PhiX174 circular single-stranded virion DNA substrate (5,386 nucleotides, New England Biolabs), was mixed with MRE11-RAD50 together with BSA or CtIP in reaction buffer (30 mM potassium-MOPS, pH 7.2, 1 mM dithiothreitol, 1 mM ATP, 25 mM KCl and 5 mM of either MgCl<sub>2</sub> or MnCl<sub>2</sub>). After incubation for 3 h at 37 °C, nuclease reactions were terminated by adding 1/10 volume of stop solution (3% SDS, 50 mM EDTA) and samples were run in a 0.8% agarose gel (1 $\times$  TAE) for 90 min at 100 mA. DNA species were stained with SYBR Gold Nucleic Acid Gel Stain (Molecular Probes) for 20 min and visualized with a fluoroimager (FLA-5000, Fujifilm).

**Homologous recombination assay.** A U2OS clone with the integrated homologous recombination reporter DR-GFP was generated as described previously<sup>39</sup>. Two days after transfection with siRNA, U2OS DR-GFP cells were co-transfected with an I-SceI expression vector (pCBA-I-SceI) together with a vector expressing monomeric red fluorescent protein (pCS2-mRFP). The latter plasmid was added in 1:3 ratio to mark the I-SceI-positive cells. Cells were harvested two days after I-SceI transfection and subjected to flow cytometric analysis to examine recombination induced by double-strand breakage. Only mRFP-positive subpopulations of cells were analysed for homologous recombination efficiency to circumvent possible differences in transfection efficiencies. Fluorescence-activated cell sorting data were analysed with CellQuest software to reveal the percentage of GFP-positive cells relative to the number of transfected cells (mRFP positive). The data were then related to a control siRNA treatment in each individual experiment. The dividing line between GFP (homologous recombination) positive and negative cells was set to 1% of the background level of GFP-positive cells in every internal control (not transfected with I-SceI). This gate was then applied to the mRFP/I-SceI positive counterparts to determine homologous recombination efficiency (see Supplementary Fig. 5b).